BNL-209524-2018-PUCP

Visualizing effective potentials and using the IBM-Q to study quantum field theory models in 0+1 dimensions

C. Kane, M. McGuigan

Submitted to the 2018 New York Scientific Data Summit (NYSDS): Data-Driven Discovery in Science and Industry Conference
to be held at Upton, NY
August 06 - 08, 2018

November 2018

Computational Science Initiative

Brookhaven National Laboratory

U.S. Department of Energy

USDOE Office of Science (SC), Advanced Scientific Computing Research (SC-21)

DISCLAIMER

Visualizing effective potentials and using the IBM-Q to study quantum field theory models in 0+1 dimensions

1st Christopher Kane
Physics Department
Syracuse University
Syracuse, United States
cfkane@syr.edu

2nd Michael McGuigan
Computational Science Initiative
Brookhaven National Lab
Upton, United States
mcguigan@bnl.gov

***Abstract*—This work explores the utility of two novel techniques applied to studying quantum field theory, namely quantum computing and visualizing effective potentials. We studied the ground state properties of the anharmonic oscillator and the Wess-Zumino model using the variational quantum eigensolver algorithm. We performed calculations for three and four qubit systems using IBM's open source quantum computing simulation software. Using effective potentials, we study a simple dark matter system with a Higgs and dark Higgs like particle interacting through a porthole fermion.**

***Index Terms*—quantum field theory, quantum computing, variational quantum eigensolver, effective potentials**

I. Introduction

Quantum field theory (QFT) is the mathematical framework that combines special relativity and quantum mechanics into one consistent theory. Although past computational tools have produced results which agree with experiment, a class of problems remain unexplored by standard techniques due to the mathematical complexity of the theory. Two novel techniques that show potential for helping solve a new class of problems are quantum computing, and visualizing effective potentials. Because these techniques are still in their infancy, we apply them to simple systems to explore their utility. We will begin with quantum computing and then move on to effective potentials.

II. Quantum Computing

A. Introduction to Quantum Computing

The concept of a quantum computer was proposed by Paul Benioff in 1980 [1], and Richard Feynman in 1982 [2]. The proposed devices are computers that use quantum systems as bits to store information. These quantum bits (qubits) experience purely quantum mechanical phenomena, e.g. superposition and entanglement, which can be leveraged to provide speedups compared to classical computers. Analogous to how classical computers use logic gates to manipulate bits, quantum computers use quantum gates to manipulate qubits. Quantum circuits are used to visualize the gates being used in a calculation. The quantum circuits we use in our calculations can be found in the appendix.

IBM is one of the world leaders in developing research grade quantum computers using superconducting circuits as qubits. Through their Quantum Experience program, IBM developed an application program interface that allows the public access to their quantum computers, Python libraries, example code, and software to simulate quantum computers classically.

Their example code was used in [3] to calculate the ground state energy of a hygrogen molecule using the Variational Quantum Eigensolver (VQE) algorithm. We modified their example code to study QFT in 0+1 dimensions using the VQE. We studied the anharmonic oscillator and the Wess-Zumino model, using three and four qubits to represent the systems. All results were obtained using the simulation software, and in principle, could be reproduced using a quantum computer.

B. Systems Studied

1) Anharmonic Oscillator: The anharmonic oscillator extends the idealized harmonic oscillator through the addition of a nonlinear term in the potential. This nonlinear term resembles the self interaction term present in the Higgs potential, and is therefore a relevant starting model to study using the VQE. The Hamiltonian for this system in terms of the fields is

$$\hat{H}_{anh} = \frac{1}{2}\hat{\pi}^2 + \frac{1}{2}\hat{\phi}^2 + \lambda\hat{\phi}^4. \tag{1}$$

Working in the energy basis, the Hamiltonian is

$$\hat{H}_{anh} = \hat{a}^\dagger\hat{a} + \frac{1}{2} + \lambda(\hat{a} + \hat{a}^\dagger)^4, \tag{2}$$

where $\hat{a}^\dagger$ and $\hat{a}$ are the creation and annihilation operators, respectively. The strength of the self interaction term is tuned by the value of the anharmonic coupling λ.

To pick an appropriate trial function, we followed a similar procedure followed in [4], where they study the structure of

This work was done as a part of the Science Undergraduate Laboratory Internship program at Brookhaven National Laboratory.

the Hamiltonian to guess a trial state. Instead of studying the Hamiltonian, we studied the properties of the ground state wavefunction directly by solving the Schrödinger equation using Mathematica.

The ground state wavefunctions of the two and three qubit systems, for $\lambda = 0.1$, are shown in (3) and (4), respectively.

$$\psi_0 = (0.998 \quad 0 \quad -0.081 \quad 0)^\intercal \tag{3}$$

$$\psi_0 = (0.998 \quad 0 \quad -0.070 \quad 0 \quad -0.008 \quad 0 \quad 0.005 \quad 0)^\intercal \tag{4}$$

We see that every other entry is zero. To generate the exact wavefunction, we therefore need $\frac{n^2}{2}$ variable parameters, where n is the number of qubits. Looking further, we see the first entry is close to one, and the nonzero entries get smaller the farther down in the vector they are located. Because we cannot continue to solve the Schrödinger equation for arbitrarily large systems, we assume this general trend will continue for all system sizes. With this information, we pick the trial function to be

$$\psi_{trial} = \begin{pmatrix} \cos\theta & 0 & \sin\theta & 0 & 0 & \cdots & 0 \end{pmatrix}^\intercal, \tag{5}$$

for both the 3 and 4 qubit case. This trial function, although it does not have enough parameters to meet the exact groundstate wavefunction, offers a significant advantage. This state can be generated through a single Y-rotation gate, providing a low depth quantum circuit which will minimize the systematic errors associated with quantum decoherence. A visual representation of the quantum circuit can be found in the appendix.

We studied the anharmonic oscillator using 3 and 4 qubits, using the above ψ_{trial} for values of λ ranging from zero to three. The error in the upper bound set by the VQE for different anharmonic couplings can be seen in fig. 1. We see that the error grows steadily as λ is increased.

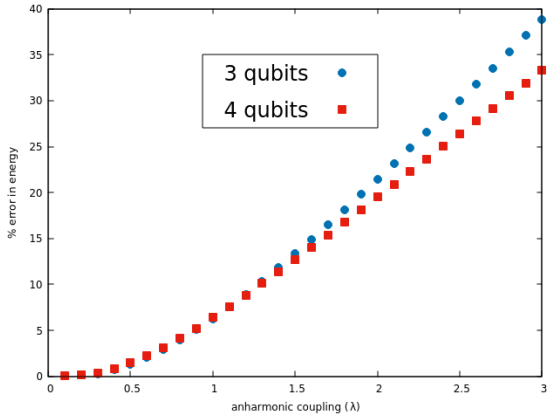

Fig. 1. This plot shows the percent error in the energy calculated by the VQE for various values of the anharmonic coupling (λ). This was done using 3 and 4 qubits to represent the Hamiltonian, using the trial wavefunction found in (5) for both cases. We notice the error is below 2% for $\lambda < 0.5$.

2) Wess-Zumino Model: The Wess-Zumino model is a model that realizes supersymmety (SUSY) [5]. SUSY is a theory that describing physics beyond the Standard Model. The theory predicts each boson (fermion) particle has an associated fermion (boson) superpartner. The Hamiltonian for the Wess-Zumino model is given by

$$\hat{H} = \frac{1}{2}\hat{\pi}^2 + \frac{1}{2}W'^2 + \frac{1}{2}[\hat{\psi}^\star, \hat{\psi}]W'', \tag{6}$$

where W is the superpotential. We chose the superpotential to be

$$W = \frac{m}{2}\phi^2 + \frac{g}{3}\phi^3, \tag{7}$$

which leads to the Hamiltonian being

$$\hat{H} = \frac{1}{2}\hat{\pi}^2 + \frac{1}{2}(m\hat{\phi} + g\hat{\phi}^2)^2 + \frac{1}{2}m[\hat{\psi}^\star, \hat{\psi}] + 2g\hat{\phi}[\hat{\psi}^\star, \hat{\psi}]. \tag{8}$$

This superpotential was chosen because it produces a Yukawa coupling between the boson and the fermion, which is a common coupling seen in QFT. This SUSY Hamiltonian also contains anharmonic terms, previously studied in [6] and a finite temperature study was performed by [7]. Again, working in the energy basis, the Hamiltonian is

$$\hat{H} = \hat{a}^\dagger\hat{a} + gm(\hat{a} + \hat{a}^\dagger)^3 + \frac{1}{2}g^2(\hat{a} + \hat{a}^\dagger)^4 + \hat{c}^\dagger\hat{c} + g(\hat{a} + \hat{a}^\dagger)(\hat{c}^\dagger\hat{c} - \hat{c}\hat{c}^\dagger). \tag{9}$$

where $\hat{c}^\dagger$ and $\hat{c}$ are the creation and annihilation operators, respectively, for the fermion.

We look to the ground state wavefunction as before, for direction when choosing our trial state. The ground state for the 2 and 3 qubit cases, for $g = 0.1$, can be found in (10) and (11), respectively.

$$\psi_0 = \begin{pmatrix} 0 & 0.999 & 0 & 0.035 \end{pmatrix}^\intercal \tag{10}$$

$$\psi_0 = (0 \quad 0.999 \quad 0 \quad -0.034 \quad 0 \quad 0.001 \quad 0 \quad -0.029)^\intercal \tag{11}$$

Like the anharmonic case, every other entry is zero, thus $\frac{n^2}{2}$ parameters are required to generate the exact wavefunction. One nontrivial difference is that consecutive nonzero entries do not fall off in magnitude like the anharmonic case. Looking at (11), the magnitude of the last entry is larger than the nonzero entry before it. After a variety of trial functions attempting to only approximate the wavefunction, all energy results from the VQE were over one-hundred percent error. This system requires a more complicated trial function because we can no longer simply neglect all but the first two nonzero terms. We resorted to a trial function that contained a parameter for each nonzero entry. Although for current quantum computers, the depth required for these trial states may be too great, it serves as proof of concept that a quantum computer is capable of producing accurate energies using the VQE for boson fermion

systems. The trial circuits for the 3 and 4 qubit states can be found in the appendix.

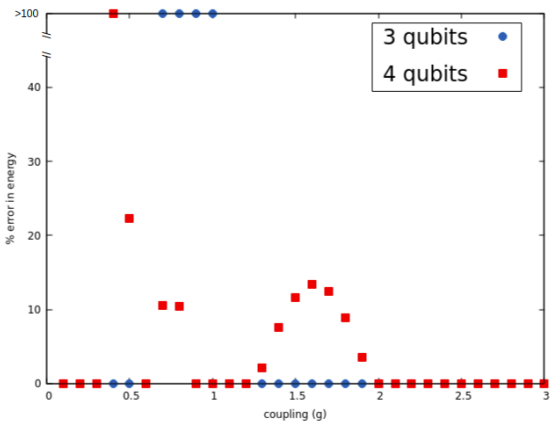

Fig. 2. This plot shows the percent error in the energy calculated by the VQE for various values of the coupling (g). This was done using 3 and 4 qubits to represent the Hamiltonian, using the trial circuit found in the appendix. We notice the error follows a hit or miss trend, either producing the exact energy or an error unacceptable by classical standards.

The results can be seen in fig. 2. We see the energies follow a hit or miss pattern for varying coupling g. The VQE either produces the exact energy, or an energy far from the exact solution, with no apparent logical pattern.

C. Discussion

For the anharmonic case, we were able to approximate the ground state wavefunction with a simple trial state, neglecting all but the first two nonzero terms. The general trend seen in fig. 1 shows that this approximation gradually becomes invalid as the anharmonic coupling λ grows. This occurs because the nonzero terms neglected by the trial state grow with λ, and therefore the quality of the approximation diminishes. Comparing these results with the SUSY case in fig. 2, we notice several differences. Firstly, we see exact energies are produced for some values of g. This is because we have parameters to account for each nonzero entry in the groundstate wavefunction. However, for some values of g, we produce errors greater than one-hundred percent. Being built out of only sine and cosine terms, the trial function is unable to account for the distribution of nonzero values. Due to the poor overlap with the exact wavefunctions, we produce upper bounds with large error.

III. Effective Potentials

A. Introduction to Effective Potentials

In QFT, because of Heisenberg's Uncertainty Principle, the quantum vacuum is not simply empty space, but rather it is teeming with virtual particle-antiparticle pairs popping into and out of existence. This phenomena generates fluctuations that change the shape of the classical potential of a system. Effective potentials account for these quantum fluctuations and how they change the classical potential. One example is the Coleman-Weinberg Potential [8], which calculates the effective potential for boson fields. Effective potentials can be extremely complicated, making it difficult to deduce properties of your system without visualizing it.

Effective potentials also can be used to express one field in terms of other fields present in the system, therefore eliminating a degree of freedom (dof) from the potential. In a visualization, these dropped dof's can be replaced with more interesting parameters in a system, therefore providing insight as to how this parameter alters the potential of a system.

The potential we study is an interaction predicted by a simple dark matter model in 3+1 dimensional QFT. Using Mathematica's 3D visualization tools, we plot the Coleman-Weinberg effective potential with varying interaction strength, and are able to determine qualitative properties of the stability of the system.

B. The Potential

The interaction we investigate describes a Higgs boson and a dark Higgs boson, each interacting with a fermion, but not directly with each other. The classical potential for this system is

$$V_{cl} = m_h^2\phi_h^2 + \frac{\lambda_h}{4}\phi_h^4 + m_d^2\phi_d^2 + \frac{\lambda_d}{4}\phi_d^4 + m_f\bar{\psi}\psi + Y(\phi_h+\phi_d)\bar{\psi}\psi, \tag{12}$$

where the h, d, and f indices represent the Higgs, dark Higgs, and fermion terms, respectively. The Y term is the Yukawa coupling strength, the λ terms are the strength of the self coupling for the boson fields, and the ϕ_R is a renormalization scale (we set $\phi_R = 1$). Following the procedure from [9], the effective potential is found to be

$$\begin{aligned} V_{eff} = {} & m_h^2\phi_h^2 + \frac{\lambda_h}{4}\phi_h^4 + m_d^2\phi_d^2 + \frac{\lambda_d}{4}\phi_d^4 \\ & + \frac{1}{64\pi^2}(2m_h + 3\lambda_h\phi_h^2)^2 \ln\frac{2m_h+\lambda_h\phi_h^2}{\phi_R} \\ & + \frac{1}{64\pi^2}(2m_d + 3\lambda_d\phi_d^2)^2 \ln\frac{2m_d+\lambda_d\phi_d^2}{\phi_R} \\ & - \frac{1}{64\pi^2}Y^4(\phi_h+\phi_d)^4 \ln\frac{Y^2(\phi_h+\phi_d)^2}{\phi_R^2}, \end{aligned} \tag{13}$$

Comparing the classical and the effective potentials, we see several differences. Firstly, we notice the fermion fields have been completely removed, and their effect rewritten in terms of the boson fields. The effective potential has reduced the dof's in the potential from four $(\bar{\psi}, \psi, \phi_h, \phi_d)$ to two (ϕ_h, ϕ_d). Secondly, we notice cross terms in the effective potential, e.g. $(\phi_h+\phi_d)^4$ and $(\phi_h+\phi_d)^2$, which represent interactions between the boson fields. These cross terms are the original interactions with the fermion, simply rewritten completely in terms of the boson fields. The effective potential has shown that two bosons interacting separately with the same fermion leads to interactions with each other. Looking naively at the classical potential does not tell us this information.

Because there are now only two dof's, we can visualize the effect of varying the strength of the Yukawa coupling without being forced to fix the value of the fermion field. Fig. 3 shows the shape of the effective potential plotted against the boson fields (ϕ_h, ϕ_d), for varying values of the Yukawa coupling. With no coupling (top left), the system is completely stable, with any perturbation leading back to equilibrium. As the coupling is increased (top right), we notice that large enough perturbations will push the system out of equilibrium. Finally, when the coupling becomes too large (bottom), the system is unstable to a perturbation of any size. This type of insight into the model could not have been easily extracted from (13). Additionally, a 3D plot would not have been possible without the fermion fields being rewritten in terms of the boson fields.

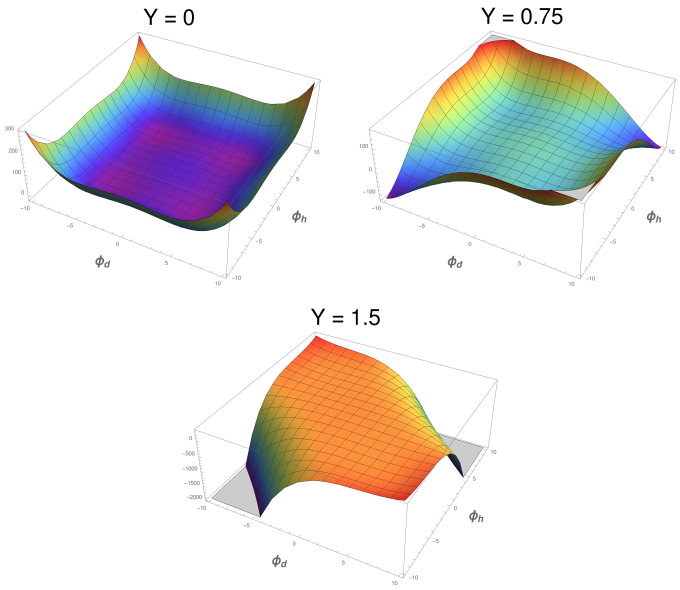

Fig. 3. Effective potential plotted against the boson fields (ϕ_1, ϕ_2), for varying values of the Yukawa coupling. Top Left: $Y = 0.0$. Top Right: $Y = 0.75$. Bottom: $Y = 1.5$. For no coupling, the system is stable. As the coupling strength is increased, the system becomes less stable, until it becomes completely unstable to any perturbation.

IV. Conclusion

In this paper, we used the VQE to calculate the ground state energies for the anharmonic oscillator, and the Wess-Zumino model in 0+1 dimensional QFT. We studied systems represented with three and four qubits. For the anharmonic oscillator, we have shown the same simple trial function is capable of producing accurate energies for small couplings (λ), for both the three and four qubit case. Alternatively, the the Wess-Zumino model not only required more complicated trial functions, but different trial functions for the three and four qubit cases. Exact energies for most values of the coupling (g) were produced for both cases. From this work, we see the large jump in complexity of using the VQE when adding more particles to a system. In future works, we would like to consider an alternative algorithm known as quantum phase estimation, and compare its scaling with particle number versus the scaling of the VQE.

Through visualizing effective potentials, we were able to determine properties of the stability of a simple system describing dark matter interacting with regular matter. These insights would have remained undiscovered without first calculating the effective potential, and then using 3D visualization techniques to study the shape of the effective potential for varying Yukawa coupling strength (Y). We aim to study more complicated systems using effective potentials in the future.

There is also the possibility that effective potentials can be used to simplify quantum computations. Each quantum particle is represented by a matrix, which is then in turn represented with qubits, where the entire quantum state is built up with tensor products [10]. Using effective potentials to eliminate degrees of freedom would lead to needing less qubits to describe the same system, therefore simplifying the trial state necessary to produce accurate energies. In the future, we hope to apply effective potentials to the Wess-Zumino model, and determine the advantages and disadvantages of each representation of the potential for study using the VQE.

Acknowledgment

This project was supported in part by the U.S. Department of Energy, Office of Science, Office of Workforce Development for Teachers and Scientists (WDTS) under the Science Undergraduate Laboratory Internships Program (SULI). I would also like to thank Eugene Dumitrescu from Oak Ridge National Lab for useful discussions regarding quantum computing. Lastly I would like to thank my mentor, Michael McGuigan, for his patience and guidance. Michael McGuigan is supported from DOE HEP Office of Science DE-SC0019139: Foundations of Quantum Computing for Gauge Theories and Quantum Gravity.

References

[1] P. Benioff, "The computer as a physical system: A microscopic quantum mechanical hamiltonian model of computers as represented by turing machines," *Journal of Statistical Physics*, vol. 22, pp. 563–591, May 1980.

[2] R. P. Feynman, "Simulating physics with computers," *International Journal of Theoretical Physics*, vol. 21, pp. 467–488, Jun 1982.

[3] A. Kandala, A. Mezzacapo, K. Temme, M. Takita, M. Brink, J. Chow, and J. Gambetta, "Hardware-efficient variational quantum eigensolver for small molecules and quantum magnets," *Nature*, vol. 549, Sep 2017.

[4] N. Klco, E. F. Dumitrescu, A. J. McCaskey, T. D. Morris, R. C. Pooser, M. Sanz, E. Solano, P. Lougovski, and M. J. Savage, "Quantum-Classical Computations of Schwinger Model Dynamics using Quantum Computers," 2018.

[5] B. Zumino and W. J., "Supergauge transformations in four dimensions," *Nuclear Physics B*, vol. 70, pp. 39–50, Feb 1974.

[6] Y. R. Musin, "A supersymmetric anharmonic oscillator," *Izvestiya Vysshikh Uchebnykh Zavedenii*, pp. 32–37, April 1988.

[7] A. Das, "Supersymmetry and finite temperature," Oct 1988.

[8] S. Coleman and E. Weinberg, "Radiative corrections as the origin of spontaneous symmetry breaking," *Phys. Rev. D*, vol. 7, pp. 1888–1910, Mar 1973.

[9] M. D. Schwartz, *Quantum Field Theory and the Standard Model*. 2014.

[10] P. Woit, *Quantum Theory, Groups and Representations: An Introduction*. 2017.

APPENDIX

A. Quantum Circuits

Quantum circuits are tools to visualize the collection of gates utilized in a calculation. Each qubit q_i has a line associated with it, and gates acted on that qubit appear on that line. Gates are implemented from left to right. Control gates are multi-qubit gates, that only perform an operation on a qubit if the control qubit is in the 1 state. They are represented by a normal gate, connected to another qubit with a line. The qubit with the dot is the control qubit. For our trial circuits, we only use NOT (X), Y-rotation (R_y), and Controlled Rotation ($Cu3$) gates. The parameter θ represents the rotation angle applied by that quantum gate.

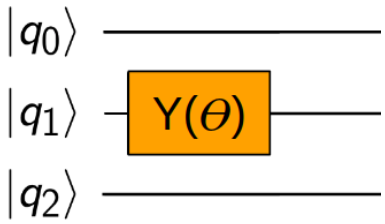

Fig. 4. This figure shows the quantum circuit used to create the trial state used in the VQE for the three qubit representation of the anharmonic oscillator. It is a very simple quantum circuit, consisting only of one Y-rotation gate.

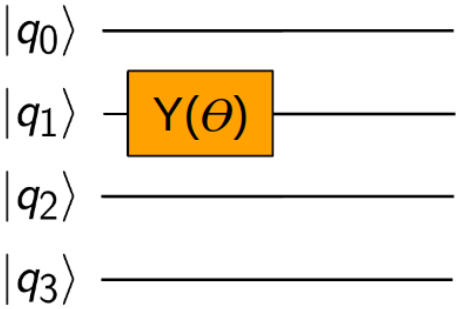

Fig. 5. This figure shows the quantum circuit used to create the trial state used in the VQE for the four qubit representation of the anharmonic oscillator. It is identical to the quantum circuit used in the three qubit case, consisting only of one Y-rotation gate.

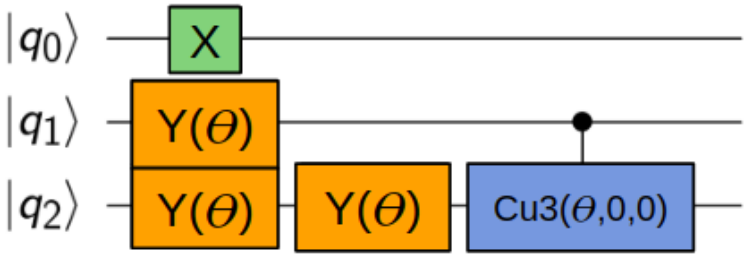

Fig. 6. This figure shows the quantum circuit used to create the trial state used in the VQE for the three qubit representation of the Wess-Zumino model. It is a more complicated trail function that either of the anharmonic cases, requiring one NOT gate, three Y-rotation gates, and one controlled rotation gate.

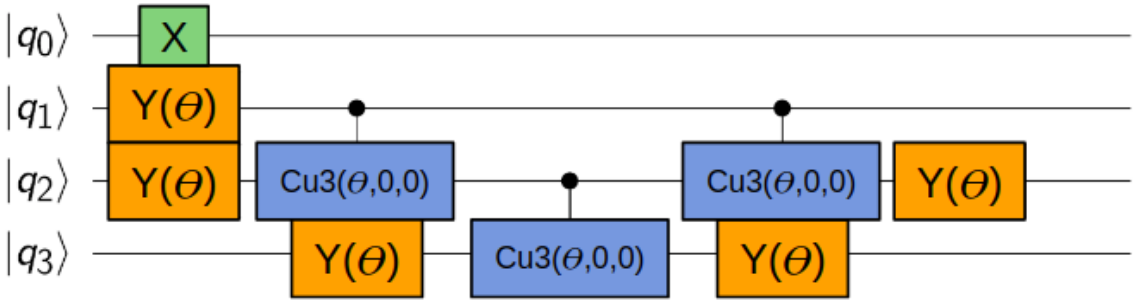

Fig. 7. This figure shows the quantum circuit used to create the trial state used in the VQE for the four qubit representation of the Wess-Zumino model. It is noticeably more complex than the three qubit case, requiring one NOT gate, five Y-rotation gates, and three controlled rotation gates.